

1 **TITLE:**
2 Counting Proteins in Single Cells with Addressable Droplet Microarrays
3

4 **AUTHORS:**
5 Chatzimichail, Stelios*
6 Institute of Chemical Biology,
7 Department of Chemistry,
8 Imperial College London,
9 London, SW7 2AZ UK
10 stelios.chatzimichail11@imperial.ac.uk
11

12 Supramaniam, Pashiini*
13 Institute of Chemical Biology,
14 Department of Chemistry,
15 Imperial College London,
16 London, SW7 2AZ UK
17 pashiini.supramaniam12@imperial.ac.uk
18

19 Ces, Oscar
20 Institute of Chemical Biology,
21 Department of Chemistry,
22 Imperial College London,
23 London, SW7 2AZ UK
24 o.ces@imperial.ac.uk
25

26 Salehi-Reyhani, Ali
27 Institute of Chemical Biology,
28 Department of Chemistry,
29 Imperial College London,
30 London, SW7 2AZ UK
31 ali.salehi-reyhani@imperial.ac.uk
32

33 *These authors contributed equally to this work.
34

35 **CORRESPONDING AUTHOR:**
36 Ali Salehi-Reyhani
37 (ali.salehi-reyhani@imperial.ac.uk)
38

39 **KEYWORDS:**
40 Droplet microfluidics, single cell protein analysis, heterogeneity, microfluidics, droplets, absolute
41 quantification, p53, cell size
42

43 **SHORT ABSTRACT:**
44 Here we present addressable droplet microarrays (ADMs), a droplet array based method able to

45 determine absolute protein abundance in single cells. We demonstrate the capability of ADMs to
46 characterize the heterogeneity in expression of the tumor suppressor protein p53 in a human
47 cancer cell line.

48

49 **LONG ABSTRACT:**

50 Often cellular behavior and cellular responses are analyzed at the population level where the
51 responses of many cells are pooled together as an average result masking the rich single cell
52 behavior within a complex population. Single cell protein detection and quantification
53 technologies have made a remarkable impact in recent years. Here we describe a practical and
54 flexible single cell analysis platform based on addressable droplet microarrays. This study
55 describes how the absolute copy numbers of target proteins may be measured with single cell
56 resolution. The tumor suppressor p53 is the most commonly mutated gene in human cancer,
57 with more than 50% of total cancer cases exhibiting a non-healthy p53 expression pattern. The
58 protocol describes steps to create 10 nL droplets within which single human cancer cells are
59 isolated and the copy number of p53 protein is measured with single molecule resolution to
60 precisely determine the variability in expression. The method may be applied to any cell type
61 including primary material to determine the absolute copy number of any target proteins of
62 interest.

63

64 **INTRODUCTION:**

65 The goal of this method is to determine the variation in abundance of a target protein in a cell
66 population with single cell resolution. Single cell analysis provides a number of benefits that are
67 not available with traditional ensemble biochemical methods.¹⁻⁵ Firstly, working at the single cell
68 level can capture the rich heterogeneity of a cell population that would otherwise be lost by the
69 averaging that occurs with traditional ensemble biochemical techniques. The majority of work-
70 horse biochemical methods work with the bulk, requiring, as they often do, millions of cells to
71 produce a result. Of course, the consequences of assessing entire cell populations depends on a
72 number of factors, for example, the heterogeneity in protein expression where some important
73 features of the distribution of protein abundance may be missed. From a practical perspective,
74 the sensitivity required of single cell techniques make them capable of working with amounts of
75 biological material that is insufficient for even the more sensitive bulk techniques to function. A
76 key example of this is the study of rare cell types such as circulating tumor cells (CTCs) where
77 even for patients with a poor prognostic outlook less than 10 CTCs might be present in a single
78 7.5 mL blood draw.⁶ Here we present the methodology required to perform single cell protein
79 measurements using a reduced volume antibody-based assay employing oil capped droplets
80 printed on an antibody microarray.

81

82 Microfluidic droplet platforms are high throughput, able to generate thousands of droplets per
83 second, and capable of isolating, and even culturing, single cells in individual droplets to perform
84 a wide array of biochemical assays. Droplet-based techniques are well suited for single cell
85 analysis,⁷⁻⁹ with notable recent examples including DropSeq¹⁰ and inDrop¹¹, which have been
86 greatly aided by the power of amplification techniques. The limited amount of material and no
87 methods of amplification for proteins make single cell proteomics especially challenging.

88

89 Droplets may be analyzed by a number of methods and fluorescence microscopy has been widely
90 used. Single molecule techniques such as total internal reflection fluorescence (TIRF) microscopy
91 allows fluorescent molecules to be visualized with unparalleled signal-to-noise ratio.¹² Due to the
92 exponential decay of the evanescent field, only fluorophores in high proximity to the surface
93 (order of 100nm) are excited making TIRF a good strategy in detecting small amounts of a target
94 molecule in a complex mixture. The inherent optical sectioning strength of TIRF also helps to
95 avoid wash steps and limits assay time and complexity. However, TIRF requires planar surfaces
96 and examples of TIRF microscopy applied to droplets in flow involve the formation of a planar
97 surface of which to image.¹³ To this end, single cell proteomic techniques often design
98 microfluidic chips around surface-immobilized capture agents in a microarray format.^{4,14}

99
100 The droplets, themselves, may be formed in arrays on planar surfaces, so-called droplet
101 microarrays.¹⁵⁻¹⁷ Spatially organizing droplets into arrays allows them to be conveniently
102 indexed, easily monitored over time, individually addressed and, if required, retrieved. Droplet
103 microarrays can achieve a high density of micro-reactors with thousands of elements per chip
104 which are either free-standing or supported by microwell structures.¹⁸⁻²⁰ They may be formed by
105 sequential deposition by liquid handling robots, inkjet spotters, contact microarrayers²¹⁻²⁶ or
106 they can self-assemble on surfaces such as superhydrophilic spots patterned on a
107 superhydrophobic surface.²⁷⁻²⁹

108
109 With these considerations in mind, Addressable Droplet Microarrays (ADMs) were designed to
110 combine the versatility, spatial addressability and reduced volumes of droplet microarrays with
111 the sensitivity of single molecule TIRF microscopy to quantitatively measure protein abundance.⁵
112 ADMs enable single cell analysis forming a droplet microarray containing single cells over an
113 antibody microarray, which is then capped with oil to prevent evaporation. The volumes of the
114 droplets are discrete to prevent sample loss, which would otherwise be achieved by on-chip
115 valving in continuous flow microfluidics.³⁰ The absolute amount of target protein from a single
116 cell is extremely small; however, the reduced volume of the droplets allows for relatively high
117 local concentration in order that they are detected using a sandwich antibody assay – antibody
118 is immobilized in a distinct region, or spot, on a surface which captures protein which in turn
119 binds to a fluorescently labelled detection antibody present in the droplet volume. As a label-
120 free approach (i.e. protein targets do not need to be labelled directly), ADMs are generally
121 applicable to analyzing cells from primary sources, such as processed blood, fine needle aspirates
122 and dissociated tumor biopsies, as well as cells from culture and their lysates.

123
124 Measuring the variation in protein abundance across a cell population is important in
125 determining the heterogeneity in response, for example, to a drug and will help in providing
126 insight into cellular functions and pathways, assessing subpopulations and their behavior as well
127 as identify rare events that would otherwise be masked by bulk methods. This protocol describes
128 how to produce and use addressable droplet microarrays to quantitatively determine the
129 abundance of the transcription factor p53 in human cancer cells and may be used to investigate
130 the role of p53 in response to chemotherapeutic drugs. The target protein is determined by the
131 choice of capture and detection antibodies and may be modified to include more or different
132 targets. Instructions are provided to build a simple apparatus incorporating a concentric nozzle

133 from general lab consumables to manually array 10 nL droplets capped with oil. The full
134 experimental process is described whereby each droplet is then loaded with a single cell, which
135 is then lysed and the expression of protein determined with single molecule resolution using TIRF
136 microscopy.

137

138 **PROTOCOL:**

139

140 **1. Preparation**

141 **1.1. Make chips and print antibody microarrays**

142 1.1.1. Attach an adhesive silicone/acrylic isolator to a coverslip functionalized to support an
143 antibody microarray. This is referred to as the chip.

144 **NOTE:** Various surface chemistries have been tested for their suitability with addressable
145 droplets.⁵ Surface chemistries may need to be optimized for alternative capture agents. ADM
146 isolators are available commercially or may be produced by laser cutting acrylic (CAD file for
147 isolator used in this work is provided as a download).

148 1.1.2. Switch on the microarrayer and set the humidity to 75%.

149 **NOTE:** Relative humidity reduces evaporation of printing solution from the microarray pin and
150 reduces intra- and inter-spot variation.

151 1.1.3. Clean the microarray pin in pin cleaning solution for 5 min by ultrasonication. Rinse the
152 pin with ultra-pure water using a wash bottle and dry using nitrogen.

153 **NOTE:** Suspend the pin as to only immerse the pin tip. A microscope slide with an appropriately
154 drilled set of holes will help if a pin holder cannot be obtained.

155 1.1.4. Make 5 mL of print buffer comprising of 3 × saline-sodium citrate (SSC) buffer, 1.5 M
156 betaine supplemented with 0.01% sodium dodecyl sulfate (SDS). Store at 4 °C indefinitely.

157 1.1.5. To prepare a printing solution, thaw anti-p53 antibody (p53/Mdm2 ELISA kit; see the
158 Table of Materials) aliquots stored at -80 °C. Mix it 1:1 with print buffer to a final concentration
159 of 0.5 mg/mL. Load 5-10 µL of printing solution in a 384 well-plate using a micropipette and place
160 in the microarrayer.

161 1.1.6. Load chips assembled in step 1.1.1 into the microarrayer. Program the microarrayer to
162 print spots at coordinates defined by the center of each well of the isolator.

163 **NOTE:** Microarrayers employ a range of, predominantly, proprietary software and so the reader
164 is encouraged to consult the relevant literature. The microarray required for the ADM isolator
165 featured in the accompanying CAD file in step 1.1.1 comprises of rectangular elements; the
166 relevant distances are provided.

167 1.1.7. Store the chips in airtight containers and wrap with foil. Store at 4 °C up to 6 weeks.

168 **NOTE:** The foil is to prevent any photo-damage. Storage at 4 °C limits the degradation rate of
169 biomolecules and any deleterious reactions that may act to reduce microarray activity. An airtight
170 container allows chips to equilibrate to room temperature before use without condensation
171 forming on the chip surface. Contact microarray printing exploits surface tension and adhesion
172 between the print solution and the print substrate to produce spots. Pre-printing or blotting is
173 normally required to remove excess solution from the microarray pin to yield uniformly sized
174 spots. Do not discard the sacrificial pre-print coverslip since it can be used to assess batch quality.

175 **1.2. Prepare syringes, tubing and concentric nozzle for dispensing addressable droplets**

176 1.2.1. Disassemble 100 µL (for the aqueous droplet) and 1 mL (for the capping oil) glass Hamilton
177 syringes and rinse parts with distilled H₂O.

178 1.2.2. Feed a 100 mm length of 150 µm ID/360 µm OD fused silica tubing through a 40 mm
179 length of 1.0 mm ID/1/16" OD PFA tubing until it protrudes by 2 mm. This will form the concentric
180 nozzle.

181 1.2.3. Apply a thin layer of cyanoacrylate glue to the end of a 10 µL pipette tip and insert into
182 the 40 mm piece of 1.0 mm ID/1/16" OD PFA tubing. If required, reposition the fused silica tubing
183 to maintain a 2 mm protrusion at the nozzle before the adhesive sets.

184 1.2.4. Insert the other end of the fused silica capillary into the end of a 200 mm length of 0.014"
185 ID/0.062" OD PTFE tubing and connect this to a 100 µL Hamilton syringe filled with 4% bovine
186 serum albumen (BSA) in phosphate-buffered saline (PBS) (PBSA).

187 **NOTE:** Proteins and other biochemical species may non-specifically bind to surfaces and can be
188 lost or denatured. BSA is used to 'block' surfaces to minimize non-specific binding by sacrificially
189 binding to those surfaces.

190 1.2.5. Insert a 400 mm length of 1.0 mm ID/2.0 mm OD FEP tubing into a 200 µL pipette tip until
191 it forms a seal. Apply a thin layer of cyanoacrylate glue to another 200 µL pipette tip and push
192 this into the first tip to fix the tubing in place. Connect the open end of the 1.0 mm ID/2.0 mm
193 OD FEP tubing to a 1 mL Hamilton syringe filled with mineral oil.

194 1.2.6. Insert the 200 µL pipette tip assembly into the 10 µL pipette tip of the concentric nozzle.

195 1.2.7. Place the syringes in separate syringe pumps as they will need to be operated
196 independently.

197 1.2.8. Fill the 100 µL syringe with 4% PBSA blocking solution. Reattach and flush the 'aqueous'
198 tubing with the blocking solution. Repeat twice for a total of 3 flushes.

199 1.2.9. Fill the 100 µL syringe with detection antibody in 4% PBSA and re-attach tubing. Replace
200 blocking solution in tubing by dispensing 25 µL detection antibody solution.

201 1.2.10. Flush the 'oil' tubing with mineral oil until all tubing and the nozzle fills with oil. Refill the
202 1 mL syringe with mineral oil and re-attach tubing.

203 1.2.11. Secure the tubing and nozzle assembly to an XYZ manipulator.

204 **1.3. Prepare microinjector and micromanipulator**

205 **NOTE:** Steps below make specific reference to components of the microinjector and
206 micromanipulator apparatus specified in the Table of Materials, but are generally applicable to
207 any such apparatus.

208 1.3.1. Assemble the microinjector by attaching the pressure tubing and the capillary holder.

209 1.3.2. Slowly rotate the piston dial until the mineral oil completely fills the line.

210 1.3.3. Mount the capillary holder into the translation head mount.

211 1.3.4. Fix the capillary in the capillary holder with the grip head.

212 1.3.5. Pipette a solution of 4% PBSA into one of the wells of the isolator.

213 1.3.6. Translate using the micromanipulator and immerse the tip of the capillary into the
214 solution.

215 1.3.7. Slowly fill the capillary with 4% PBSA and leave to block for 10 min.

216 1.3.8. Eject the microcapillary and swivel the translation module so that the assembly is clear of
217 the chip.

218 **2. Form Addressable Droplets and Load with Single Cells**

219 **2.1. Form addressable droplets**

220 2.1.1. Secure the chip on the microscope stage.

221 **NOTE:** The microscope is an inverted fluorescence automated microscope capable of single
222 molecule TIRF fitted with an an encoded XY stage and an electron multiplying charge-coupled
223 device camera (EM-CCD).

224 2.1.2. Record the microscope stage coordinates of each spot in the array using the automated
225 microscope control software.

226 2.1.3. Set the XYZ manipulator on the microscope stage. Place the nozzle at an angle of 50-60°.
227 Ensure that the nozzle has sufficient length and clearance to reach the chip.

228 2.1.4. Set the 'aqueous' and 'oil' syringe pumps to dispense 10 nL at 100 $\mu\text{L}/\text{min}$ and 5 μL at 100
229 $\mu\text{L}/\text{min}$, respectively.

230 Note: During preparation, the aqueous solution at the head of the nozzle may dry.

231 2.1.5. Dispense aqueous solution until a bead of fluid is visible at the head of the nozzle. Dab
232 with a dust free wipe to remove it.

233 Note: Depending on the number of conditions under investigation, reserve a number of wells to
234 serve as reservoirs for cells. For a single cell line/type a single reservoir will suffice.

235 2.1.6. Using the automated microscope control software, set the microscope stage coordinates
236 to an antibody spot in the array and focus on the coverslip surface.

237 2.1.7. Careful not to disturb the spot, using the XYZ manipulator, align the glass capillary tip of
238 the concentric nozzle to the side of the antibody spot and dispense 10 nL of aqueous solution.

239 2.1.8. Without moving the stages, dispense 5 μ L of oil to cap the aqueous solution.

240 2.1.9. Slowly raise the nozzle clear of the droplet and move to the next well.

241 2.1.10. Repeat steps 2.1.7-2.1.9 for all antibody spots in the array.

242 2.1.11. After 30 min, image all spots in the array using the automated microscope control
243 software to determine the background of single molecules bound to each antibody spot prior to
244 loading cells.

245 **2.2. Load addressable droplets with cells**

246 2.2.1. Remove the cell culture flasks from the incubator and detach cells.

247 **NOTE:** In this study, the BE human colon carcinoma cell line was used and cultured using
248 Dulbecco's Modified Eagles Medium (DMEM) supplemented with 10% (v/v) foetal bovine serum
249 (FBS) in a CO₂ incubator.

250 2.2.2. If required, fluorescently stain cells.

251 2.2.3. Resuspend cells in a solution of 0.125 μ g/mL detection antibody (anti-p53 antibody (DO-
252 1) labelled with Alexa 488) in 10% FBS in L-15 media.

253 2.2.4. Ensure a single cell suspension by running the cell solution through a 40 μ m pitch cell
254 strainer.

255 2.2.5. Count cells using a hemocytometer and dilute or concentrate the cell solution to a
256 concentration of 25-400 $\times 10^3$ cells/mL. This ensures that cells sediment with sufficient spacing
257 to comfortably manipulate the microcapillary.

258 2.2.6. Load single cells into addressable droplets from the cell reservoir using the
259 micromanipulator and microcapillary.

260 Note: Non-adherent cells may be loaded in bulk into the micropipette and dispensed one by one
261 into addressable droplets. Despite surface blocking treatment, adherent cell lines will tend to
262 non-specifically stick to the glass microcapillary inner wall and be lost.

263 2.2.7. Using a 10× objective to observe, use the microinjector to aspirate a single cell into the
264 microcapillary from the cell reservoir.

265 2.2.8. Store the micromanipulator stage coordinates if using an electronic manipulator stage or
266 manually note the z-position.

267 2.2.9. Retract the micropipette by translating it upwards to clear the 1 mm height of the chip.
268 Perform this manually with a joystick or automatically using the 'Eject' feature of an electronic
269 manipulator stage.

270 2.2.10. Set the stage coordinates to that of an addressable droplet the using automated
271 microscope control software.

272 2.2.11. 'Inject' the micropipette by returning it to the stored (or noted) z-position. Perform this
273 manually with a joystick or automatically if using an electronic manipulator stage.

274 Note: The microcapillary will pierce the capping oil and be located within the aqueous portion of
275 the addressable droplet.

276 2.2.12. Dispense the cell in the addressable droplet using the microinjector. The volume of a 10
277 nL addressable droplet will increase by less than 1%.

278 2.2.13. Repeat 2.2.7-2.2.12 for the remaining addressable droplets leaving some free for the
279 experimental control where addressable droplets do not contain a cell.

280
281 **NOTE:** A simpler alternative to loading single cells into addressable droplets using a microcapillary
282 and micromanipulator is to replace the solution in step 1.2.9 with a solution of detection antibody
283 in 4% PBSA containing cells at a concentration on the order of 10^5 cells/mL, equivalent to 1 cell/10
284 nL. Single cell occupancy will be Poissonian and the cell concentration will need to be optimized.

285
286 **2.3. Lyse cells and image array**

287 2.3.1. Image cells in droplets using brightfield microscopy, including any fluorescence imaging.

288 **NOTE:** Imaging takes approximately 3 min to image ~100 droplets using an automated
289 microscope.

290 2.3.2. Image all spots in the array using single molecule TIRF microscopy.

291 Note: These images will be subsequently analyzed in section 3 to determine the background of
292 single molecules bound to each antibody spot prior to lysis. Single molecule imaging using total

293 internal reflection fluorescence (TIRF) microscopy takes approximately 5 min to image ~100
294 spots.

295 2.3.3. Focus on a cell in an addressable droplet and optically lyse.

296 2.3.3.1. Achieve complete optical lysis of single cells by focusing a single 6 ns laser pulse
297 close to the location of the cell (laser wavelength used here 1064 nm and pulse energies are 14.1
298 $\pm 0.3 \mu\text{J}$ per pulse).

299 Note: The laser pulse sets up an expanding cavitation bubble that shears the cell and liberates
300 cellular constituents into the droplet volume.^{4,31} The mechanical processes due to laser-induced
301 lysis do not disturb the oil–water interface at low pulse energies. Optical lysis typically takes
302 approximately 20-30 min to lyse 100 cells. As discussed in the Discussion section, there are a
303 number of alternative methods to lyse single cells if optical lysis setup is not possible.

304 2.3.4. Repeat for all cell-containing addressable droplets leaving 5 free for the experimental
305 control where addressable droplets contain an un-lysed cell.

306 2.3.5. Note the time at which each cell is lysed.

307 Note: These times will be used to correct individual binding curves for each spot in step 3.1.9.
308 Often it is sufficient to note the times when the first and last cells are lysed and estimate the rest
309 assuming an adequately consistent time between lysis events.

310 2.3.6. Acquire single molecule images using TIRF microscopy of all spots every 10 min for the
311 first 30 min then every 20 min for a further 60 min. If only interested in the amount of protein
312 bound at equilibrium, image all spots after incubating the chip for 90 min at room temperature.

313 **NOTE:** The time to reach equilibrium will depend on the droplet volume and the affinities of the
314 antibodies used in the assay. TIRF microscopy is performed using a laser excitation source at $\lambda =$
315 488 nm and 1.5 mW power as measured at the back aperture using an optical power meter.
316 Single molecule images are acquired by setting the acquisition settings on the EM-CCD camera
317 to 900 ms acquisition time, 16-bit digitization at 1 MHz readout rate and an EM gain factor of 10.
318 The isolator may be re-used by carefully removing the coverslip.

319 **3. Data Analysis**

320 **3.1. Single molecule counting (non-congested/digital regime)**

321 3.1.1. Using Fiji or Matlab, for any non-congested antibody spot, load the image acquired before
322 lysis (background, BKD).

323 **NOTE:** The operations in the following steps are straightforwardly performed using Fiji image
324 analysis software. A user guide may be found at the following link
325 <https://imagej.nih.gov/ij/docs/guide/146.html>.

326 3.1.2. Duplicate BKD and Gaussian blur the duplicate with a 50 pixel radius.

327 3.1.3. Flatten the BKD image so that there is an effective uniform intensity distribution of the
328 excitation light source by dividing the BKD image by the blurred BKD image, producing BKD_FLAT.

329 3.1.4. Subtract each pixel in the image by 1. The average pixel intensity should be 0.

330 **NOTE:** Field flattening and flattened background images may be checked easily since the sum of
331 all pixels should be 0 and any offset may be more straightforwardly compensated for.

332 3.1.5. Select a 50 pixel × 50 pixel area in any of the 4 corners of the BKD_FLAT image and
333 measure the pixel intensity standard deviation (σ). This determines *off-spot* background where
334 there is unlikely to be a high density of single molecules.

335 3.1.6. Set the image threshold to 3σ and create a binary image SM_MASK, where pixels whose
336 value are below the threshold are set to zero and pixels exceeding the threshold are set to 1.

337 Note: The threshold will determine the confidence with which thresholded pixels belong to a
338 single molecule.

339 3.1.7. In the segmented image SM_MASK, set pixel intensity values to zero of any objects that
340 do not have a size of 4-9 pixel² and a circularity of 0.5 – 1.

341 **NOTE:** The pixel size may need to be optimized for other fluorophores and microscope set ups.
342 Due to the type of camera noise single pixels may be above this threshold and not be discarded
343 despite not being single molecules. The pixel size criterion will correctly discard such pixels. Single
344 molecules are generally circular in shape. A circularity value of 1 indicates a perfect circle whereas
345 a value approaching 0 indicates an increasingly elongated shape. The remaining objects are single
346 molecules and may be counted. A mask may be set to demarcate the area of the spot to
347 discriminate *on-spot* and *off-spot* counts per frame. This is easier for frames acquired at later
348 times when there is a sufficient signal on-spot which can then be applied to earlier frames.

349 3.1.8. For the same non-congested antibody spot, load and repeat steps 3.1.1 – 3.1.7 for all
350 image frames captured as a time-resolved series acquired post lysis. Use the lysis times noted in
351 step 2.3.5. to correct any binding curves.

352 **3.2. Single molecule counting (congested/analogue regime)**

353 3.2.1. In order to calculate the average intensity of a single molecule, repeat steps 3.1.1 – 3.1.8.

354 3.2.2. Multiply the images BKD_FLAT and SM_MASK to produce an image whereby non-zero
355 pixel values are associated with single molecules.

356 3.2.3. Sum all pixel intensity values and divide by the number of counted single molecules as
357 per step 3.1.8.

358 3.2.4. For any congested antibody spot, load the image acquired post-lysis and flatten with a
359 blurred background image as per steps 3.1.2 and 3.1.3.

360 3.2.5. Subtract each pixel in the flattened image by 1.

361 3.2.6. Select a 50 pixel × 50 pixel area in any of the 4 corners of the image and measure the pixel
362 intensity standard deviation (σ).

363 3.2.7. Create a binary image mask by setting the image threshold to 3σ and set pixel intensity
364 values to zero of any objects with a size less than 4 pixel^2 .

365 3.2.8. Multiply the flattened congested antibody spot image by the binary image mask.

366 3.2.9. The sum of the remaining pixel intensities.

367 3.2.10. Divide the sum of pixel intensities by the average single molecule intensity to calculate
368 the number of single molecules bound to the congested spot.

369 **3.3. Calibration curve for absolute quantification**

370 3.3.1. Partially repeat steps 1 and 2 by forming 10 nL addressable droplets with the detection
371 antibody in 4% PBSA solution spiked with a known concentration recombinant protein.

372 3.3.2. Perform a concentration series of $10^2 - 10^7$ recombinant proteins per droplet.

373 3.3.3. Use this data to calibrate any single molecule counts per spot to protein abundance per
374 droplet and by extension protein abundance per single cell.

375

376 **REPRESENTATIVE RESULTS:**

377 The absolute basal protein copy number of p53 was determined with single cell resolution in a
378 human colon cancer cell line, BE cells. We demonstrate how p53 expression can vary over several
379 orders of magnitude and show a weakly positive correlation between cell size and protein copy
380 number within the resting BE cell population.

381

382 Addressable Droplet Microarrays are formed when aqueous droplets are dispensed at antibody
383 spot locations and capped with oil. Here, the droplets support a sensitive p53 protein assay.
384 Coverslips are arrayed with capture antibody spots using a contact microarrayer and a pin. The
385 anti-p53 capture antibody is taken from a commercial ELISA test kit. The printing conditions were
386 such that capture spots were approximately $100 \mu\text{m}$ in diameter with a maximum capture
387 capacity of $6.2 \pm 0.5 \times 10^5$ proteins per spot.³²

388

389 The use of an isolator bonded to the coverslip allows a higher density of droplets to be formed
390 since it limits the spread of oil to nearby antibody capture spots. In each well of the isolator
391 droplets are formed by dispensing an aqueous solution which is then capped with oil to prevent
392 evaporation (**Figure 1A**). A minimal amount of oil may be dispensed to cap the droplet; however,
393 it is useful to dispense an amount which fills each isolator well exactly such that the oil surface is

394 flat for imaging. Isolators are either commercially sourced or made by laser cutting acrylic sheets.
395 Silicone isolators are available pre-cut wells in a 4 × 6 array (n = 24) but may be modified to a 4 ×
396 11 array (n = 44) using a biopsy or multi-hole leather punch. The laser cut isolator in **Figure 1B**
397 shows an array of 100 hexagonal wells each with a maximal diameter of 2.89 mm, a center-to-
398 center separation of 3.9mm and a height of 0.5mm. The droplets may be stored and remain
399 stable for extended periods of time (observed up to 3 months).

400
401 Droplets are created manually using a home-built apparatus which translates a concentric tubing
402 nozzle (**Figure 1C**) which is connected to two syringe pumps (**Figure 1A**). The concentric tubing
403 nozzle is comprised of a fused silica capillary, which dispenses the aqueous phase, fed through a
404 short length of PEEK tubing, which dispenses the oil phase. Using a microscope, the nozzle is
405 aligned to an antibody spot and the pumps would first dispense the aqueous solution
406 immediately followed by the oil (**Figure 1E**, steps 1-4). Once all droplets in the ADM are formed,
407 a microinjector and micromanipulator (CellTram Vario and PatchMan NP2; Eppendorf, Germany)
408 are used to load each droplet with a single cell (**Figure 1D**). The micropipette would capture a cell
409 from a reservoir of cells, dispensed in one of the wells on the chip, be translated to a droplet well
410 and then penetrate the oil cap to deliver the cell into the aqueous droplet (**Figure 1D**, steps 5-8).

411
412 All spots within the droplets are imaged prior to lysis and will be used to determine the degree
413 of non-specific binding to the spots (**Figure 2A**). Single cells are fully lysed (including nucleus)
414 using optical methods.³¹ Optical lysis relies on the shearing force of an expanding laser pulse-
415 induced cavitation bubble to disrupt the cells. Care must be made that the oil-water interface
416 not be disturbed by these processes by limiting the pulse energies and depositing cells away from
417 the oil/water interface. Once cells are lysed, the array is imaged by TIRF microscopy using an
418 automated microscope; frames are acquired every 10 min for 30 min and then every 20 min for
419 a further 60 min. The conditions, such as antibody affinity, protein diffusion and droplet volume,
420 are such that binding equilibrium is reached within the 90 min acquisition. A typical single cell
421 pulldown is shown in **Figure 2A**.

422
423 The process of image analysis to determine the single molecule counts is schematically depicted
424 in **Figure 2B**. Images of spots are either considered to be non-congested, where target protein
425 concentration is such that single molecules are well separated and easily distinguished, or
426 congested, where target protein concentration is higher and single molecule images overlap and
427 are no longer individually distinguishable. Since the TIRF excitation profile is uneven, it is crucial
428 that all acquired images be flat-field corrected. A Gaussian blur is applied to a non-congested
429 frame which acts as a smoothing filter to remove detail and noise and produce an image with the
430 average profile of the TIRF excitation profile. This processed image may be used to 'flatten' the
431 original image. For non-congested images, where, even at equilibrium, there are few single
432 molecules, a frame may be processed to correct itself. This approach is not applicable to a
433 congested spot, where single molecules densely occupy the spot and requires a background
434 image to be acquired for flattening. Flattened frames are then thresholded for pixels with
435 intensities at least 3 times the background standard deviation plus its mean value. Single
436 molecules are then automatically detected by identifying 4-9 clustered pixels with a circularity
437 greater than 0.5 using the Particle Analysis features of Fiji. From the results, the average intensity

438 of a single molecule may be calculated. It is used to determine the number of single molecules
439 on a congested spot by dividing the antibody spot total intensity by the known average intensity
440 of a single molecule. These steps may be automated using Fiji's script editor.

441
442 A concentration series is performed to determine the single molecule count at equilibrium in the
443 droplets with known concentrations of recombinant p53 protein (**Figure 3A**). The conditions are
444 such that the capture antibody spots capture a fraction of the total target protein, approximately
445 1% in the region of linearity (for 10^5 - 10^8 proteins per droplet $R^2 = 0.99$). The level non-specific
446 binding in the droplets is 187 ± 60 molecules. The results of the single cell pulldowns may then
447 be converted to achieve distributions of absolute protein copy number per cell. **Figure 3B** shows
448 the distribution of absolute p53 protein expression in single BE cells using ADMs. P53 protein
449 expression in the BE cells, which may be assumed to be genetically identical or very similar, is a
450 stochastic process. The distribution is Gamma-like - asymmetric and unimodal with a long tail.
451 Consequently, the mean (1.82×10^6 proteins) can overestimate the modal protein abundance
452 (bin 0 - 5.0×10^5 proteins), and the standard deviation (1.88×10^6 proteins) doesn't fully capture
453 the features of the distribution. This distribution is an example of the importance of single cell
454 measurements to capture the heterogeneity of protein expression in the cell population which
455 would otherwise be lost when averaging with bulk measurements. Additional parameters for
456 each cell may be measured. Here, the cell volume is estimated by measuring each cell diameter
457 prior to lysis in the droplet and assuming the cell is approximately spherical. **Figure 3C** shows a
458 comparison of p53 absolute protein copy number in single BE cells as a function of cell size. There
459 is a tendency for larger cells to have a higher total p53 copy number. Interestingly, it is possible
460 from the distribution that there is coordination between p53 expression and cell size since there
461 appears to be a minimum p53 copy number per cell; however, the mechanisms by which this
462 arises requires further investigation.

463
464 **Figure Legends:**

465 **Figure 1: Addressable Droplet Microarray Apparatus and Chip.** a) Droplets are dispensed
466 manually using a 3-axis manipulator to translate a concentric tubing nozzle. The aqueous droplet
467 is dispensed at specific locations in an antibody microarray followed by a capping oil. b) The
468 isolator enables a higher density of addressable droplets on the substrate by limiting the spread
469 of the oil. Isolators may be produced by laser cutting 0.5 mm acrylic sheets. To aid visualization
470 of the droplets, blue food coloring dye is deposited using the apparatus in a). Scale bar 10 mm,
471 inset scale bar 1 mm. c) The concentric tubing nozzle allows addressable droplets to be formed,
472 assembled as in step 1.2 of the protocol. d) A microinjector and micromanipulator are used to
473 isolate cells into individual addressable droplets, prepared as in step 1.3 of the protocol. e) The
474 major steps in the process of creating and loading addressable droplets is shown. An antibody
475 spot is located using an encoded translation stage (1) where the tip of the capillary tubing is
476 aligned (2) and the aqueous (3) then oil (4) components are dispensed. Single cells may be loaded
477 using a glass microcapillary (5-8) which can repeatedly address the aqueous droplet (7) and
478 deposit a cell (8). Scale bars 100 μm . The red arrow in (5) and (8) highlights the isolated single cell
479 and the inset of (8) shows the isolated single cell at high magnification (scale bar 10 μm). Portions
480 of this figure has been modified from ¹², reproduced by permission of The Royal Society of
481 Chemistry.

482

483 **Figure 2: Image analysis steps.** Each spot in the array is periodically imaged by TIRF microscopy
484 until equilibrium (t_{Eq}) is reached (90 min for p53 assay). The equilibrium time depends on t in
485 solution as well as the affinities of the antibodies' pair for the targeted protein. a) Example single
486 molecule TIRF microscopy images of the background as well as an example single cell pulldown
487 (scale bars 20 μm). Inset image shows a magnified portion of the background image with some
488 single molecules highlighted by red arrows (scale bar 5 μm). b) Outline of image analysis detailed
489 in step 3 of the protocol. Briefly, there are two broad regimes where the spots may be considered
490 non-congested, single molecules are sparse, and congested, where the density of single
491 molecules is such that there is significant overlap and may no longer be singly identifiable. Steps
492 may be straightforwardly automated in ImageJ to analyze the data. A crucial step in image
493 analysis is field flattening the images to remove the effect of the excitation laser profile.

494

495 **Figure 3: Single cell data.** Absolute quantification is achieved using a calibration curve. a) Single
496 molecule counts are made using known concentrations of recombinant protein. This is a
497 calibration curve and is used to convert single molecule counted on each spot to number of target
498 proteins in the analysis volume and hence single cell copy number. The horizontal red dashed
499 line indicates the level of non-specific binding of 187 ± 60 molecules. The error bars are one
500 standard deviation of the mean of 3 experimental runs. The dashed line represents 100%
501 detection of protein. b) A distribution of the single cell basal p53 protein expression in BE cancer
502 cells is shown showing a long-tailed gamma-like distribution where p53 protein expression in
503 some cells is significantly higher than the modal value. c) Scatter plot of p53 protein copy number
504 per cell as a function of cell volume showing how protein expression varies as a function of cell
505 size. Portions of this figure have been modified from ¹², reproduced by permission of The Royal
506 Society of Chemistry.

507

508 **DISCUSSION:**

509 Addressable Droplet Microarrays are a sensitive and extensible method for quantitatively
510 determining the absolute copy number of protein within a single cell.

511

512 Limiting the level of non-specific binding (NSB) is critical within the protocol to achieving as low
513 a limit of detection as possible. Proteins and other biochemical species may non-specifically bind
514 to a number of interfaces present within the droplets - the coverslip surface, the antibody spot
515 and the oil/water interface. Proteins can be lost by partitioning into the interface or the oil itself.
516 We have shown that 4% BSA present in the aqueous droplet is capable of limiting NSB of proteins
517 using the antibodies specified in the protocol. Alternative protein targets and the antibodies used
518 to detect them may require alternative blocking approaches, such non-ionic detergents or
519 compatible surfactants. Fluorinated oils may also be tested for their suitability in serving as the
520 capping oil. In such cases, additional considerations such as the critical micellar concentration
521 and the density of the capping oil must be made.

522

523 The unwashed printing buffer which remains at each spot location after arraying aids in
524 alignment. When initially depositing the droplets, care must be taken to not scratch or damage
525 the antibody spot by the tip of the concentric tubing nozzle. In developing the method further, a

526 fluorescent dye may be doped into the antibody printing buffer which becomes immobilized in
527 addition to the capture antibody. This would allow for wash and blocking steps to be performed
528 prior to droplet arraying; however, such a step would not necessarily be required if using non-
529 manual methods of droplet arraying that such as inkjet printing methods.

530

531 The surface of the commercially sourced coverslips upon which droplets are formed is coated
532 with a hydrophilic polymer and the aqueous droplets produced upon them with a volume of 10
533 nL have a diameter of 751 ± 42 nm. There is a limit to how much the deposited droplet should
534 wet the surface or spreads due to the weight of the capping oil since below a minimum thickness
535 there is increased optical scatter from the TIRF excitation laser. The scatter increases the average
536 level of background and can drown out signal when detecting single molecules. The antibody
537 spot must also be located away from the droplet edge since the excitation laser light may partially
538 or fully strike an area outside of the aqueous droplet. The critical angle condition will no longer
539 be met for light striking the glass-oil interface as opposed to the glass-water interface.

540

541 To quantitatively determine the abundance of protein the number of single molecules bound to
542 a spot must be determined through image analysis. To determine the total amount of protein in
543 solution from the single molecule count a calibration curve is required and enables the technique
544 to be absolutely quantitative.

545

546 To minimize photobleaching, spots are not imaged continuously and the TIRF excitation laser
547 source power is minimized. The protocol as presented has been used successfully for photostable
548 fluorophores such as the Alexa Fluor dyes. Alternative fluorophores may be used but
549 photobleaching must be assessed and the imaging protocol adapted if necessary. The total
550 number of single molecules per frame may be plotted against time to reproduce the binding
551 curve although this is certainly not necessary if binding kinetics are not sought and imaging a
552 single frame at equilibrium will suffice.

553

554 Although there is a requirement of two high affinity antibodies, this results in a highly sensitive
555 and highly specific assay, crucial for measurements at the single cell level. The p53 antibodies
556 used in this protocol are well optimized in detecting free p53 from single cells. The target protein
557 is determined by the choice of antibodies and may be modified in a number of ways: 1, both the
558 capture and detection antibodies may be replaced to bind alternative targets; 2, the detection
559 antibody may be replaced to probe protein-protein interactions or post-translational
560 modifications to the protein bound to the capture antibody, e.g. determine the phosphorylation
561 status of captured p53; 3, multiplexed assays may be achieved by printing multiple capture
562 antibody spots in close proximity – printing a 3×3 spot array is possible within 10nL droplets. Of
563 course, for any change of target protein a number of antibody screens, controls and
564 optimizations must be undertaken.

565

566 Several methods for lysing single cells have been reported.³³ Optical lysis is a chemical-free
567 approach to rapidly lyse individual cells without altering the contents of cells and maintaining the
568 integrity of proteins and their complexes. Chemical lysis using detergents poses a problem to the
569 integrity of the droplets when using mineral oil and can interfere with interactions between

570 molecules.³⁴ However, for assays where chemical lysis is compatible it is attractive approach since
571 it is not reliant on equipment such as lasers or micropatterned electrodes.³⁵

572
573 The droplets show comparable performance with alternative single cell methods. In the current
574 generation of droplets using the suggested p53 antibodies, the level of NSB is 187 ± 60 molecules
575 per spot. The single molecule counts exhibit strong linearity ($R^2 = 0.99$) in the region spanning 10^5
576 – 10^8 recombinant p53 proteins per droplet. This suggests that while lower levels of protein may
577 be detected in cells, there is a limit of quantitation of 10^5 p53 proteins; this corresponds to a
578 single molecule count on the spots of 901 ± 83 . This is predominantly limited by the volume of
579 the droplets and adsorption to the interface. The performance of the p53 assay is such that when
580 performed in a 10 nL volume only $1.1 \pm 0.2\%$ of the total target protein is captured from solution;
581 this increases to $85 \pm 9\%$ when reducing the analysis volume to 0.2 nL.³⁶ By reducing the volume
582 of the droplets to below 1nL and reducing adsorption, there is potential using the specified
583 antibodies to p53 in improving the limit of detection to <50 proteins per cell. Therefore,
584 addressable droplets have the potential to be used to measure very low abundance proteins from
585 single cells.

586
587 The addressability of the droplets afforded by the easily penetrable oil cap permits the cell
588 analysis volume to be sequentially challenged. The use of a micropipette enables the injection of
589 a desired number of cells into each droplet in a plug of 10-20 pL, which does not significantly
590 increase the volume. For the chip shown in Figure 1B with 100 wells, to form droplets and load
591 them with single cells typically takes 75-90 min. Loading cells may also be achieved by addressing
592 the droplet using the concentric tubing nozzle instead of the micropipette or using a solution
593 containing cells when initially forming the droplets. The latter would be useful in limiting the
594 number of steps in the protocol but, in both cases, the occupancy per droplet would follow a
595 Poissonian distribution. This would limit the proportion of single cell data per chip; however,
596 droplets with zero or multiple cells would serve as controls. An additional limitation in using the
597 concentric nozzle to address droplets is the droplet volume would increase in 10nL increments.
598 With the suggested modifications above this could be improved. On-chip droplet microfluidics
599 are capable of producing droplets at high frequency and have potential in being automatically
600 combined with ADMs to produce and manipulate droplets and sequentially deposit them in a
601 planar array. This would certainly overcome the limitations in production of ADMs while also
602 enabling single molecule readout of droplets.

603
604 The ability to address each individual droplet has a range of possible uses. We have demonstrated
605 the ability to sequentially load single cells. It also permits removal of the unbound cellular
606 material post lysis and post analysis by pipette for analysis using other methods. Examples of
607 subsequent analysis would include quantitative real-time PCR or mass-spectrometry.

608
609 One of the current bottlenecks for laboratories wanting to take a quantitative approach to single
610 cell protein analysis is the high technical barrier and the need for specialized equipment. With
611 ADMs, miniaturized, high sensitivity analyses may be achieved without the need for clean room
612 facilities to fabricate microfluidic lab-on-a-chip devices. Experiments are not limited by the design
613 of the chip and their volume and position may be altered without the need for fabricating new

614 masters. Certainly, there is scope for improvement in simplifying the technique and lowering the
615 barrier to entry for single cell analysis to just a microarrayer, to print both antibody and droplet
616 microarrays, and a fluorescence microplate reader, to image.

617
618 A number of clinical applications of single cell analysis are emerging, particularly in the treatment
619 of cancer. Tumor heterogeneity is a major challenge to effective chemotherapy. In tumor
620 development, mutations arise with increasing frequency and heterogeneity can result in
621 morphological, genetic, and proteomic variability. Single cell analysis is able to resolve cellular
622 heterogeneity within a tumor and provide a platform to help better understand and predict drug
623 resistance and guide therapy.

624
625 **ACKNOWLEDGMENTS:**
626 ASR designed experiments, developed protocols and analyzed data. SC and PS performed cell size
627 experiments. ASR and OC wrote the manuscript. The authors wish to gratefully acknowledge the
628 support of Prof. David R. Klug for providing access to equipment. The authors wish to thank the
629 Imperial College Advanced Hackspace for access to fabrication and prototyping facilities.

630
631 **DISCLOSURES:**
632 The authors have nothing to disclose.

633
634 **REFERENCES**
635 1. Willison, K. R. & Klug, D. R. Quantitative single cell and single molecule proteomics for
636 clinical studies. *Curr. Opin. Biotechnol.* **24** (4), 745–751, doi:10.1016/j.copbio.2013.06.001
637 (2013).
638 2. Heath, J. R., Ribas, A. & Mischel, P. S. Single-cell analysis tools for drug discovery and
639 development. *Nat. Rev. Drug Discov.* **15** (3), 204–16, doi:10.1038/nrd.2015.16 (2016).
640 3. Eyer, K., Stratz, S., Kuhn, P., Küster, S. K. & Dittrich, P. S. Implementing enzyme-linked
641 immunosorbent assays on a microfluidic chip to quantify intracellular molecules in single cells.
642 *Anal. Chem.* **85** (6), 3280–3287, doi:10.1021/ac303628j (2013).
643 4. Salehi-Reyhani, A. *et al.* A first step towards practical single cell proteomics: a
644 microfluidic antibody capture chip with TIRF detection. *Lab. Chip.* **11** (7), 1256–1261,
645 doi:10.1039/c0lc00613k (2011).
646 5. Salehi-Reyhani, A., Burgin, E., Ces, O., Willison, K. R. & Klug, D. R. Addressable droplet
647 microarrays for single cell protein analysis. *Analyst* **139** (21), 5367–5374,
648 doi:10.1039/C4AN01208A (2014).
649 6. Cristofanilli, M., Budd, G. & Terstappen, L. Circulating tumor cells, disease progression,
650 and survival in metastatic breast cancer. *N. Engl. J. Med.* **351** (8), 781–792,
651 doi:10.1056/NEJMoa040766 (2004).
652 7. Lan, F., Haliburton, J. R., Yuan, A. & Abate, A. R. 2016 Droplet barcoding for massively
653 parallel single-molecule deep sequencing. *Nat. Commun.* **7**, 1–10, doi:10.1038/ncomms11784
654 (2016).
655 8. Ramji, R. *et al.* Single cell kinase signaling assay using pinched flow coupled droplet
656 microfluidics. *Biomicrofluidics* **8** (3), 34104, doi:10.1063/1.4878635 (2014).
657 9. He, M., Edgar, J. S., Jeffries, G. D. M., Lorenz, R. M., Shelby, J. P. & Chiu, D. T. Selective

658 encapsulation of single cells and subcellular organelles into picoliter- and femtoliter-volume
659 droplets. *Anal. Chem.* **77** (6), 1539–1544, doi:10.1021/ac0480850 (2005).

660 10. Macosko, E. Z. *et al.* Highly parallel genome-wide expression profiling of individual cells
661 using nanoliter droplets. *Cell* **161** (5), 1202–1214, doi:10.1016/j.cell.2015.05.002 (2015).

662 11. Klein, A. M. *et al.* Droplet barcoding for single-cell transcriptomics applied to embryonic
663 stem cells. *Cell* **161** (5), 1187–1201, doi:10.1016/j.cell.2015.04.044 (2015).

664 12. Reck-Peterson, S. L., Derr, N. D. & Stuurman, N. Imaging single molecules using total
665 internal reflection fluorescence microscopy (TIRFM). *Cold Spring Harb. Protoc.* **5** (3), pdb.top73-
666 top73, doi:10.1101/pdb.top73 (2010).

667 13. Chen, D., Du, W. & Ismagilov, R. F. Using TIRF microscopy to quantify and confirm
668 efficient mass transfer at the substrate surface of the chemistode. *New J. Phys.* **11** (31), 75017,
669 doi:10.1088/1367-2630/11/7/075017 (2009).

670 14. Shi, Q. *et al.* Single-cell proteomic chip for profiling intracellular signaling pathways in
671 single tumor cells. *Proc. Natl. Acad. Sci. U. S. A.* **109** (2), 419–424,
672 doi:10.1073/pnas.1110865109 (2012).

673 15. Sun, Y. *et al.* A novel picoliter droplet array for parallel real-time polymerase chain
674 reaction based on double-inkjet printing. *Lab Chip* **14** (18), 3603, doi:10.1039/C4LC00598H
675 (2014).

676 16. Jogia, G., Tronser, T., Popova, A. & Levkin, P. Droplet Microarray Based on
677 Superhydrophobic-Superhydrophilic Patterns for Single Cell Analysis. *Microarrays* **5** (4), 28,
678 doi:10.3390/microarrays5040028 (2016).

679 17. Yen, T. M. *et al.* Self-Assembled Pico-Liter Droplet Microarray for Ultrasensitive Nucleic
680 Acid Quantification. *ACS Nano* **9** (11), 10655–10663, doi:10.1021/acsnano.5b03848 (2015).

681 18. Labanieh, L., Nguyen, T. N., Zhao, W. & Kang, D. K. Floating droplet array: An ultrahigh-
682 throughput device for droplet trapping, real-time analysis and recovery. *Micromachines* **6** (10),
683 1469–1482, doi:10.3390/mi6101431 (2015).

684 19. Lee, Y. Y., Narayanan, K., Gao, S. J. & Ying, J. Y. Elucidating drug resistance properties in
685 scarce cancer stem cells using droplet microarray. *Nano Today* **7** (1), 29–34,
686 doi:10.1016/j.nantod.2012.01.003 (2012).

687 20. Popova, A. A., Demir, K., Hartanto, T. G., Schmitt, E. & Levkin, P. A. Droplet-microarray
688 on superhydrophobic–superhydrophilic patterns for high-throughput live cell screenings. *RSC*
689 *Adv.* **6** (44), 38263–38276, doi:10.1039/C6RA06011K (2016).

690 21. Chen, F. *et al.* Inkjet nanoinjection for high-throughput chemiluminescence immunoassay
691 on multicapillary glass plate. *Anal. Chem.* **85** (15), 7413–7418, doi:10.1021/ac4013336 (2013).

692 22. Zhu, Y., Zhu, L.-N., Guo, R., Cui, H.-J., Ye, S. & Fang, Q. Nanoliter-scale protein
693 crystallization and screening with a microfluidic droplet robot. *Sci. Rep.* **4**, 5046,
694 doi:10.1038/srep05046 (2014).

695 23. Sun, Y., Chen, X., Zhou, X., Zhu, J. & Yu, Y. Droplet-in-oil array for picoliter-scale analysis
696 based on sequential inkjet printing. *Lab Chip* **15** (11), 2429–2436, doi:10.1039/C5LC00356C
697 (2015).

698 24. Liberski, A. R., Delaney, J. T. & Schubert, U. S. “One cell-one well”: A new approach to
699 inkjet printing single cell microarrays. *ACS Comb. Sci.* **13** (2), 190–195, doi:10.1021/co100061c
700 (2011).

701 25. Yusof, A. *et al.* Inkjet-like printing of single-cells. *Lab a Chip - Miniaturisation Chem. Biol.*

702 **11** (14), 2447–54, doi:10.1039/c1lc20176j (2011).

703 26. Zhu, Y., Zhang, Y.-X., Liu, W.-W., Ma, Y., Fang, Q. & Yao, B. Printing 2-dimensional droplet
704 array for single-cell reverse transcription quantitative PCR assay with a microfluidic robot. *Sci.*
705 *Rep.* **5**, 9551, doi:10.1038/srep09551 (2015).

706 27. Ueda, E., Geyer, F. L., Nedashkivska, V. & Levkin, P. A. Droplet Microarray: facile
707 formation of arrays of microdroplets and hydrogel micropads for cell screening applications.
708 *Lab Chip* **12** (24), 5218–5224, doi:10.1039/c2lc40921f (2012).

709 28. Kozak, K. R. *et al.* Micro-volume wall-less immunoassays using patterned planar plates.
710 *Lab Chip* **13** (7), 1342–50, doi:10.1039/c3lc40973b (2013).

711 29. Yen, T. M. *et al.* Self-Assembled Pico-Liter Droplet Microarray for Ultrasensitive Nucleic
712 Acid Quantification. *ACS Nano* **9** (11), 10655–10663, doi:10.1021/acsnano.5b03848 (2015).

713 30. Au, A. K., Lai, H., Utela, B. R. & Folch, A. Microvalves and Micropumps for BioMEMS.
714 *Micromachines* **2** (4), 179–220, doi:10.3390/mi2020179 (2011).

715 31. Lai, H.-H. *et al.* Characterization and use of laser-based lysis for cell analysis on-chip. *J. R.*
716 *Soc. Interface* **5 Suppl 2** (Suppl_2), S113-21, doi:10.1098/rsif.2008.0177.focus (2008).

717 32. Salehi-Reyhani, A. *et al.* Scaling advantages and constraints in miniaturized capture
718 assays for single cell protein analysis. *Lab Chip* **13** (11), 2066–74, doi:10.1039/c3lc41388h
719 (2013).

720 33. Brown, R. B. & Audet, J. Current techniques for single-cell lysis. *J. R. Soc. Interface* **5**
721 **Suppl 2** (Suppl 2), S131-8, doi:10.1098/rsif.2008.0009.focus (2008).

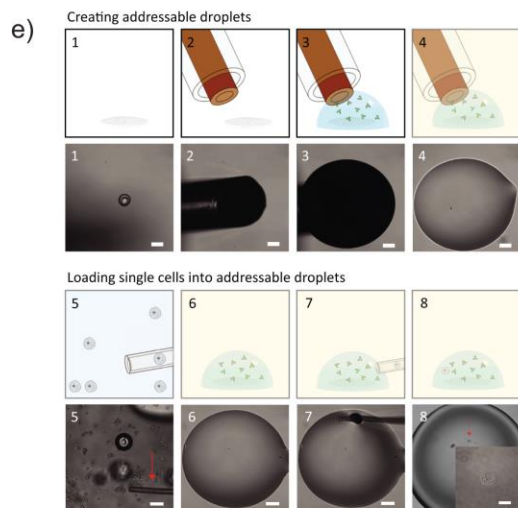
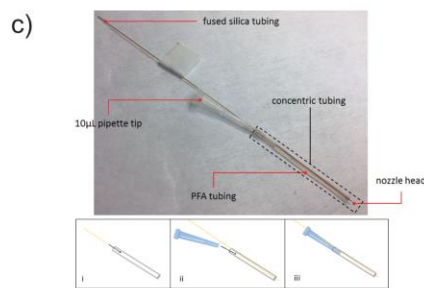
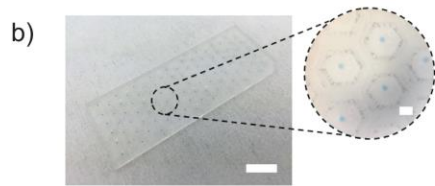
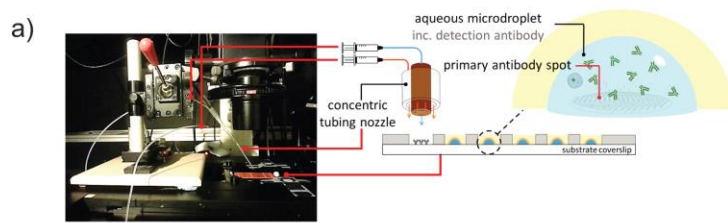
722 34. Womack, M. D., Kendall, D. A. & MacDonald, R. C. Detergent effects on enzyme activity
723 and solubilization of lipid bilayer membranes. *BBA - Biomembr.* **733** (2), 210–215,
724 doi:10.1016/0005-2736(83)90524-2 (1983).

725 35. Ramji, R., Xiang, A. C., Ying, N. J., Teck, L. C. & Hung, C. C. Microfluidic Single Mammalian
726 Cell Lysis in Picolitre Droplets. *J. Biosens. Bioelectron.* **S12** (1), 10–13, doi:10.4172/2155-
727 6210.S12-001 (2013).

728 36. Burgin, E. *et al.* Absolute quantification of protein copy number using a single-molecule-
729 sensitive microarray. *Analyst* **139** (13), 3235, doi:10.1039/c4an00091a (2014).

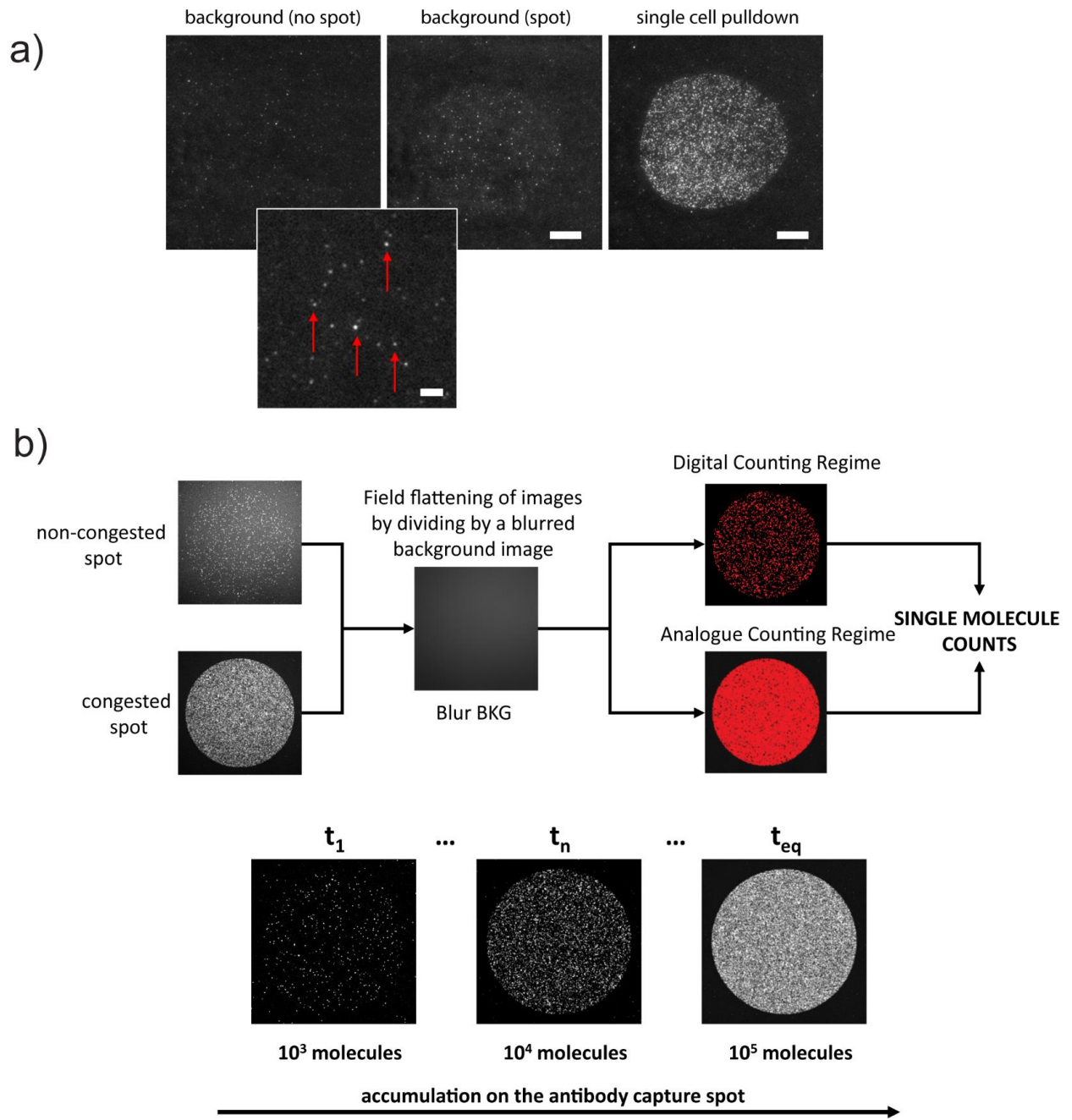
730
731
732
733
734
735
736
737
738
739
740
741
742
743
744
745

746 Figure 1

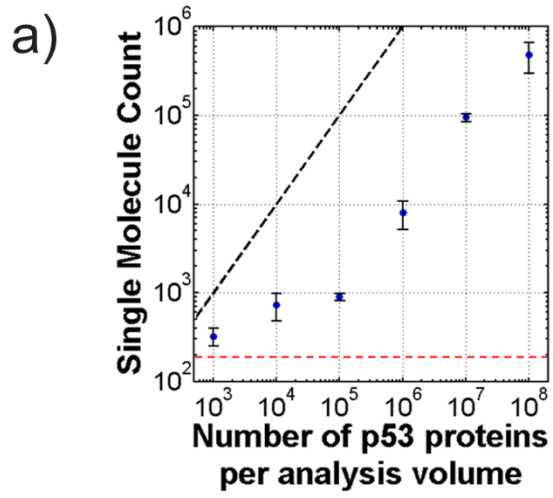


747

748 Figure 2
749



750
751
752
753
754
755
756
757
758



b) histogram of p53 protein expression in single BE cells

